Journal of Glaciology

Letter

*Present address: Department of Physical Geography, Utrecht University, Utrecht, The Netherlands

Cite this article: Kääb A, Bazilova V, Leclercq PW, Mannerfelt ES, Strozzi T (2023). Global clustering of recent glacier surges from radar backscatter data, 2017–2022. *Journal of Glaciology* **69**(277), 1515–1523. https://doi.org/10.1017/jog.2023.35

Received: 1 September 2022
Revised: 29 April 2023
Accepted: 3 May 2023
First published online: 29 June 2023

Keywords:
glacier surges; mountain glaciers; remote sensing

Corresponding author:
Andreas Kääb;
Email: kaeaeb@geo.uio.no

cambridge.org/jog

Global clustering of recent glacier surges from radar backscatter data, 2017–2022

Andreas Kääb[1], Varvara Bazilova[1,*], Paul Willem Leclercq[1], Erik Schytt Mannerfelt[1] and Tazio Strozzi[2]

[1]Department of Geosciences, University of Oslo, Oslo, Norway and [2]Gamma Remote Sensing, Gümligen, Switzerland

Abstract

Using global Sentinel-1 radar backscatter data, we systematically map the locations of glaciers with surge-type activity during 2017–22. Patterns of pronounced increases or decreases in the strongest backscatter between two winter seasons often indicate large changes in glacier crevassing, which we treat here as a sign of surge-type activity. Validations against velocity time series, terminus advances and crevassing found in optical satellite images confirm the robustness of this approach. We find 115 surge-type events globally between 2017 and 2022, around 100 of which on glaciers already know as surge-type. Our data reveal a pronounced spatial clustering in three regions, (i) Karakoram, Pamirs and Western Kunlun Shan (~50 surges), (ii) Svalbard (~25) and (iii) Yukon/Alaska (~9), with only a few other scattered surges elsewhere. This spatial clustering is significantly more pronounced than the overall global clustering of known surge-type glaciers. The 2017–22 clustering may point to climatic forcing of surge initiation.

Introduction

Glacier surging refers to strongly enhanced ice flow speeds over time-periods of months to years. The overall term glacier surging encompasses a range of magnitudes for flow acceleration, a range of time scales for active and quiescent phases and a range of suggested processes leading to acceleration (Jiskoot, 2011; Truffer and others, 2021). Knowing where and when glaciers show surge-type flow instabilities is important for a number of scientific and applied reasons: surges disturb the direct link between climate and glacier mass and length changes, and thus the climatic interpretation of them (e.g. Gardelle and others, 2013). The mechanisms of glacier surging and the conditions leading to it are still incompletely understood and the topic of a substantial body of past and ongoing research (Harrison and Post, 2003; Jiskoot, 2011; Sevestre and Benn, 2015; Benn and others, 2019; Thogersen and others, 2019; Truffer and others, 2021). Glacier surges can cause significant natural hazards, mostly through damming-up of rivers and thus causing outburst-flood hazards during their advance, but also due to direct inundation of land and damage of mountain infrastructure (Bevington and Copland, 2014; Round and others, 2017; Steiner and others, 2018; Hock and others, 2019; Muhammad and others, 2021; Truffer and others, 2021). The initiation of catastrophic low-angle glacier detachments and their huge ice-rock avalanches also appears to be connected to surge-type processes (Kääb and others, 2018; Jacquemart and others, 2020; Kääb and others, 2021). The significant crevassing that is associated with surging glaciers complicates safe travel across glaciers. Finally, questions arise whether and how climate change could impact surge initiation, frequency and magnitude, and therefore on the response of glaciers to climate change (Dunse and others, 2015; Sevestre and Benn, 2015; Yasuda and Furuya, 2015; Kienholz and others, 2017; Benn and others, 2019; Hock and others, 2019; Nuth and others, 2019).

Glacier surges are identified and mapped using a number of (often combined) indicators such as looped moraines, specific landforms in the glacier forefield, exceptional and major glacier advance, exceptional crevassing, sheared-off glacier tributaries or particular patterns of elevation change (Jiskoot and others, 2003; Grant and others, 2009; Sevestre and Benn, 2015; Farnsworth and others, 2016; Herreid and Truffer, 2016; Mukherjee and others, 2017; Guillet and others, 2022). The increasing availability of regional to global-scale measurements of repeated glacier surface velocity fields from optical or radar images, where possible combined with repeat elevation measurements, offers a good opportunity to identify glacier flow instabilities and at the same time quantify in detail the evolution of ice kinematics over entire glaciers and surge events (Copland and others, 2009; Gardelle and others, 2013; Rankl and Braun, 2016; Strozzi and others, 2017; Altena and others, 2019; Guillet and others, 2022).

Leclercq and others (2021) introduced a method to detect surge-type glacier flow instabilities through the change in backscatter that they cause in repeat satellite synthetic aperture radar (SAR) images. Here, we build on this approach and use it to map surge-type events globally over the period 2017–22. We briefly introduce and demonstrate the approach and data used, and then present and discuss our global map of recent glacier surges.

Methods and data

The increase in crevassing that is typically associated with surge-type glacier instabilities often causes strongly enhanced radar backscatter in satellite SAR images. This signal can be

enhanced by stacking repeat radar images, preferably taken from the same nominal orbit to avoid variation of topographic effects and taken over the winter season, when glaciers typically show little other backscatter change due to cold and dry conditions. A synthetic image of strongest backscatter is then created over each seasonal (or sub-seasonal) stack (Fig. 1). When comparing these individual stack maximum images over different years (here we use normalised differences, the so-called normalised difference index NDI), increased crevassing appears in our implementation bright in the grey-scaled NDI image between two years, decreasing crevassing appears dark, and areas of moderate change appear medium grey (Fig. 1). The spatial patterns of such backscatter increases or decreases are then visually interpreted to decide whether they indicate glacier surges, or other changes not of interest here. We apply the approach to the EU Copernicus Sentinel-1 C-band data archive 2017–22 as available in Google Earth Engine (Gorelick and others, 2017) and use this powerful cloud-processing platform to generate winter backscatter NDI images and manually mark the locations of surge-type events. This approach was recently introduced by Leclercq and others (2021), including more technical details, implementation, the code, tests of a number of parameterisations and validation against measured velocity time series. In sum, the approach appears reliable, detecting most independently identified surges quite robustly.

As an extension to the method in Leclercq and others (2021) we also generate minimum and maximum images of the stack of the annual backscatter NDI images, i.e. the minimum and maximum NDI over the entire 2017–22 period (panel f in Fig. 1). These overall NDI images support the finding of surge-like events in a region before going in detail into the annual backscatter NDI images in order to closer understand the temporal evolution of the surge signal. We start our dataset in 2017 because the early record of Sentinel-1 data before 2017 is incomplete (e.g. North American and Eurasian Arctic or parts of High Mountain Asia (HMA) with only few or no data). There are also some small gaps in Sentinel-1 cover during some years after 2017 and in particular in 2022 after failure of one of the two Sentinel-1 satellites in late 2021 (e.g. in the Russian Arctic), which should however have only limited impact on our global surge location map as surges are typically well visible over more than one year.

Two aspects of our approach are important to keep in mind when assessing and using the data and results. First, we interpret surges visually and mark them manually on the annual backscatter NDI images 2017–18, 2018–19, 2019–20, 2020–21 and 2021–22. While the signal appears rather clear for most cases, there are a few cases where the decision whether the changes indicate a surge or not is uncertain. To check interpretations and avoid us overlooking events, three of us independently performed the mapping that was then iterated to compile the final dataset. Second, radar backscatter changes reflect the crevassing but not other possible indicators of a surge such as elevation changes, or the magnitude of velocity changes. In that sense, our data reflect one specific type of surge definition that relies exclusively on crevassing (cf. Copland and others, 2003; Grant and others, 2009), as opposed to, for instance, a kinematic definition derived from surface velocity measurements (Guillet and others, 2022). However, we consider surge classification to be ambiguous and dependent on the method used, because surge-type glacier behaviour encompasses a continuum of temporal and spatial scales, magnitudes and processes, not all of which are well understood.

For complementing the method illustration in Figure 1, we measure time series of ice speed using standard offset tracking procedures (Strozzi and others, 2002; Paul and others, 2015) based on repeat Sentinel-1 data, for Scheelebreen complemented by repeat Sentinel-2, Landsat 8 and ICEEYE data. For an initial test of potential differences in mass balance of our surge-type glaciers compared to non-surging glaciers, we use the global dataset of elevation changes by Hugonnet and others (2021).

On the global level, we compare our data to the Randolph Glacier Inventory version 6 (RGI-Consortium, 2017), on regional levels to surge inventories for HMA by Guillet and others (2022) and for Svalbard by Farnsworth and others (2016). We also combine an extended global surge inventory from RGI v.6 surges and a number of other regional surge inventories (Jiskoot and others, 2003; Sevestre and Benn, 2015; Farnsworth and others, 2016; Bhambri and others, 2017; Goerlich and others, 2020; Guan and others, 2022; Guillet and others, 2022; Guo and others, 2022). In the following, we term this inventory RGI-extended. We clean this compilation for identical glaciers in the individual inventories but do else not check for consistency as this work is out of focus for the present study.

Results

To demonstrate our approach, we show winter-to-winter backscatter NDI images over an area in south-east Spitsbergen (Fig. 1; for other examples, see Leclercq and others, 2021). The example shows (panel a) a decreasing surge (Strongbreen) where only the tidewater front is still increasingly active, (d and e) increasing surges (d and e: Scheelebreen, first marginal crevassing 2020–21; e: Vållakrabreen, first marginal crevassing 2021–22), (d and f) increasing and decreasing surge-activity (Kvalbreen) and (a–e) a surge consisting of two phases of high activity (Arnesenbreen). The evolution of glacier surface velocities at a representative point in the lower glacier centre is very consistent with backscatter changes. Increasing velocities between two winters are reflected in increasing backscatter, and vice-versa. Slight decreases in backscatter are still found when surge velocities are already low again, indicating continued closing of crevasses at the beginning of the kinematic quiescence phase. The Scheelebreen example shows that even the onset of increases in velocities could already be seen as small increases in marginal (shear-zone) crevassing (2020–21; panel d of Fig. 1). It remains, though, to be defined from which point on backscatter (and speed) increases indicate a surge.

Supplementary Table S1 lists all surge-type events interpreted from our NDI images outside the two ice sheets. In total, we find 115 events that we interpret as surge-type in the 2017–22 Sentinel-1 backscatter data. Our global mapping procedure consumed roughly one week working time per operator. We also find clearly changing backscatter signals on a number of outlet glaciers of the Greenland ice sheet, but have not further investigated if these signals indicate exceptional flow instabilities or rather usual multiannual fluctuations of ice speed and crevassing. The in-depth analysis of these events is beyond the focus of this paper but the glacier coordinates and names of the corresponding outlet glaciers are given in Supplementary Table S3 for completeness.

In Figure 2 we plot the geographic distribution of all 115 events in our dataset. For comparison, we also show the location of all surges contained in the RGI v.6 and our extended RGI inventory. The RGI v.6 indication of surge-type glaciers (RGI surge categories 3 = observed surge, 2 = probable surge, 1 = possible surge) is based on Sevestre and Benn (2015) but omits the distinction of surges of different tributary glaciers within the same RGI glacier (RGI-Consortium, 2017).

Our 2017–22 surges appear clustered into three regions, namely (i) Karakoram, Pamirs and Western Kunlun Shan (~50 surges), (ii) Svalbard (~25) and (iii) the Kluane National Park and Reserve/St. Elias Mountains in Yukon and Alaska (~9) (Fig. 2). Other regions that contain surge-type glaciers did not

https://doi.org/10.1017/jog.2023.35 Published online by Cambridge University Press

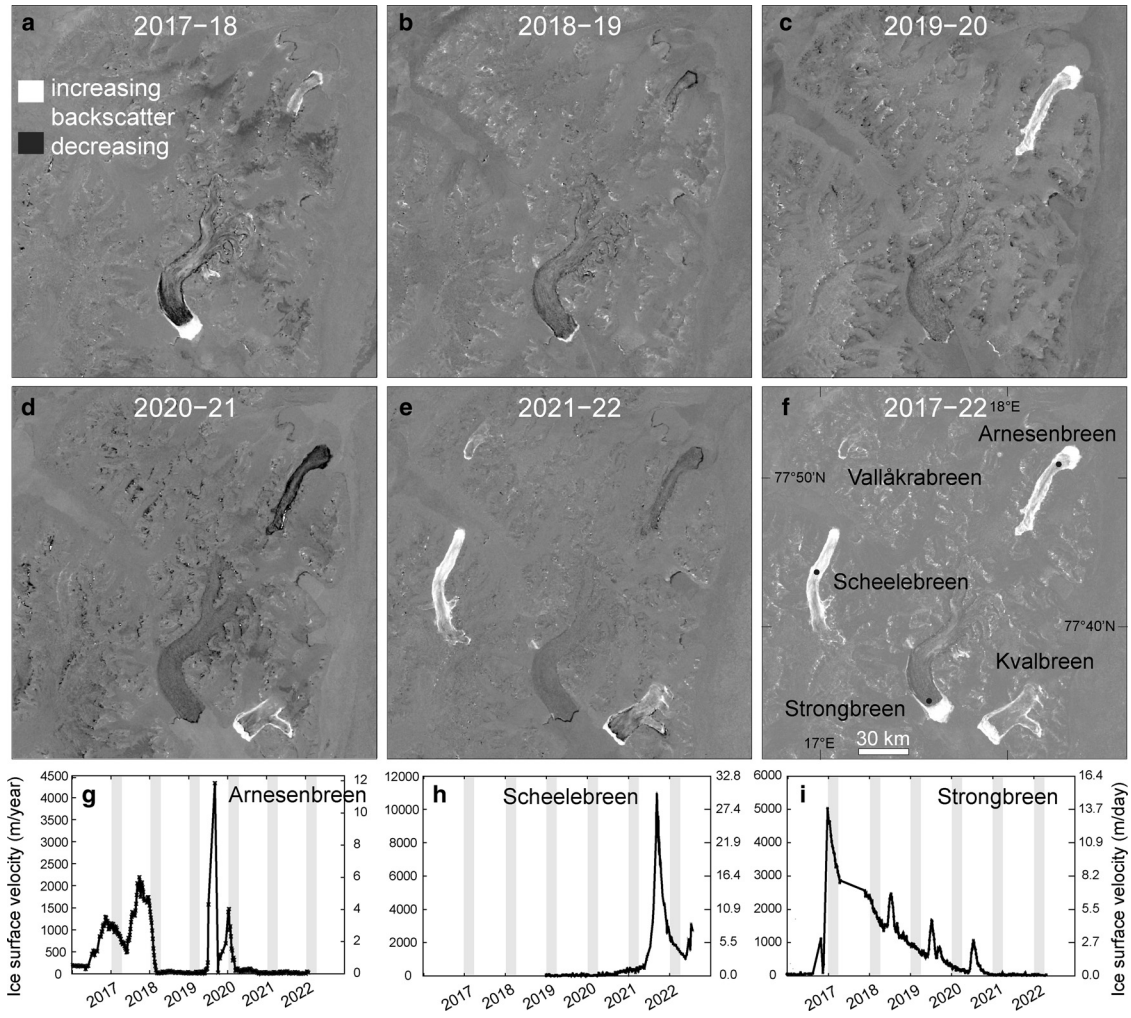

Figure 1. Examples of winter-to-winter Sentinel-1 radar backscatter changes for a region in south-east Spitsbergen, displayed as normalised differences between maximum winter backscatter of two subsequent years (a–e). Bright greyscale indicates increasing backscatter, dark greyscale decreasing backscatter over time. Increasing backscatter is interpreted as increasing crevassing and surge-type activity, and vice-versa. The middle right panel (f) shows the maximum backscatter normalised difference over the entire 5-year period and indicates the five surges observed in the area. The lowest row (g–i) shows selected comparisons to glacier surface velocity time series. The grey vertical bars in the panels of the lowest row indicate the periods over which Sentinel-1 data have been stacked for examples a–f (1 January–1 April of each year). Velocity series g–i refer to single points on the surge centre (black dots in panel f).

show glacier surges in 2017–2022, or only a few scattered ones. Within the HMA region (i), the surges are concentrated in the northern part of Pamir, the north-eastern part of Karakoram and the Western Kunlun Shan. A few surges are scattered all over the mountain ranges of HMA.

To investigate the spatial clustering more quantitatively, we choose a surging glacier and compute the distances to all other surging glaciers (example for one glacier in Fig. 3, red dots). We iterate this procedure over all surging glaciers to compute the average distance of any surging glacier to any other surging glacier and to compile a distance-dependent distribution by calculating the percentage of the sample of glaciers for which this average mutual distance is below a given distance (Fig. 3). This gives us the so-called empirical cumulative distribution function (eCDF) of distances between the different glacier samples. The procedure is run over the 115 surges derived from 2017–22 Sentinel-1 images, over the 1343 RGI v.6 surges (for the different RGI surge categories 'observed', 'probable' and 'possible' surge), our RGI-extended, and all 216'502 RGI v.6 glaciers (Fig. 3). As an example, for an average glacier, 6% of all other glaciers are located within 1000 km. Analogously, for an average RGI v.6 surge-type glacier (RGI surge flag 3), 16% of all other glaciers with observed surges (RGI surge flag 3) are located within 1000 km. For an average glacier with observed surge-type activity 2017–22, 21% of all glaciers with observed surge-type activity 2017–22 are located within 1000 km. The RGI v.6-derived surge distributions are given for the two combinations 'observed', and 'observed' + 'probable' + 'possible' surges. To interpret Figure 3, the higher a curve is on the *y*-axis the more clustered is a distribution relative to a reference distribution, such as the entire RGI v.6. Steps in the curves indicate the distinctiveness and number of clusters, with sharp steps indicating spatially separated clusters. The spatial distribution of the 2017–22 surge data appears more clustered than the reference datasets and has the most pronounced steps, i.e. clusters. Whereas the fact that surge-type glaciers are globally clustered with respect to the full global glacier sample (black line in Fig. 3) is well known (Sevestre and Benn, 2015), the important result of the present study is rather that our 2017–22 surges (red line) are globally more clustered than RGI surge-type glaciers (blue and brown lines). For illustration, we also give the distance distribution of one surging glacier (94.9 lon, 29.8 lat, south-east Asia) to all other 2017–22 surging glaciers (red dots in Fig. 3). This example glacier is chosen randomly among the glaciers from which the three main surge clusters have different overall spherical distances. For visualisation it makes the example more distinct if the distances to the main

https://doi.org/10.1017/jog.2023.35 Published online by Cambridge University Press

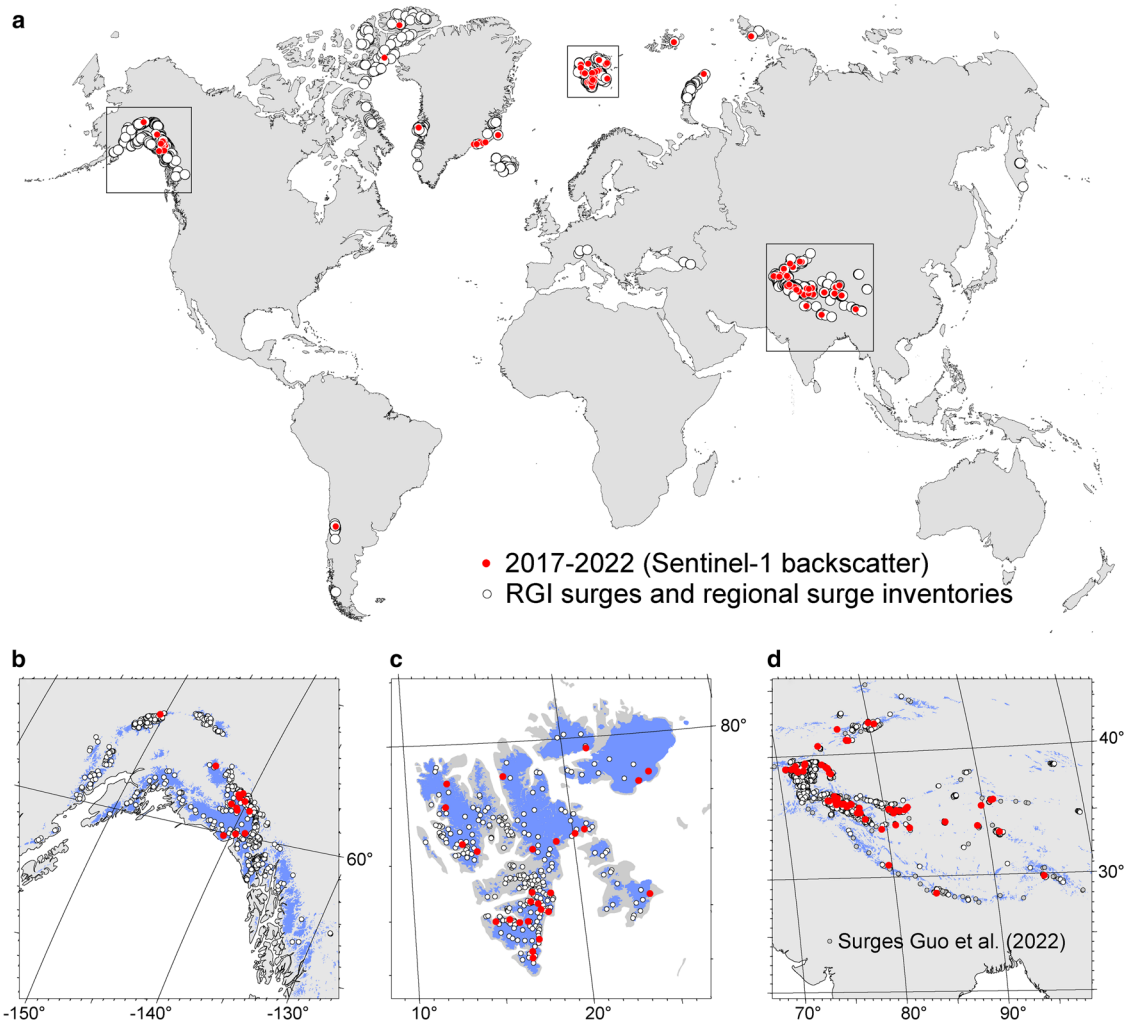

Figure 2. Maps of Sentinel-1 backscatter-derived glacier surges over 2017–22. (a) Global distribution of 2017–22 surges (red dots), and glaciers with RGI v.6 surge-type flag and additional regional inventories (white circles; see main text). (b–d) Details of the main map, including RGI v.6 glacier areas. Map projection is van der Grinten as compromise between equal-area and conformal projection.

surge clusters do not overlap for a selected glacier in the representation of Figure 3. The red curve in Figure 3 is the average of all 115 curves for the individual surging glaciers during 2017–22.

In addition to the global distribution functions (eCDFs) shown in Figure 3, we do equivalent analyses also separately for the regions Alaska/Yukon, Svalbard and HMA (Supplementary material). For Svalbard, we add a distribution based on the surge dataset by Farnsworth and others (2016), and for HMA a distribution based on the dataset by Guillet and others (2022). Guillet and others (2022) generated an inventory of 666 glaciers that surged between 2000 and 2018 in HMA, using speed variations, elevation changes and visual surge signs as indicators. We include Guo and others (2022) in Figure 2, but not in our detailed analysis as they base their surge detection purely on elevation differences, which is a very different definition compared to the one used in the present study. Farnsworth and others (2016) list 708 surge-type glaciers on Svalbard compiled from previous studies and newly mapped using land-based crevasse squeeze ridges as surge indicator. In short, the regional eCDFs of distances show that the 2017–22 glacier surges for Alaska/Yukon are more clustered than surge reference data, but that this is not the case for Svalbard and HMA.

Using two different approaches, we estimate the probability that the clustering we observe could be obtained just by random sampling. First, we add the 95% percentiles to our distance distributions, showing significant separation of the distributions for parts of distances on global level (Fig. 3), and partially for regional levels (Supplementary material). Second, we randomly sample 115 glaciers among the RGI surge-type glaciers, compute distance distributions and repeat this procedure 1000 times in a bootstrapping approach. In only 1–2% of the cases, we obtain mean and median distances equal or smaller than the ones found in our observed 2017–22 surge data, with similar numbers for both RGI v.6 and RGI-extended. Relative to the RGI surge data, both tests indicate that the global surge clustering observed over 2017–22 is statistically significant and hardly a result of random sampling. Applying the bootstrapping test regionally for Alaska/Yukon against RGI v.6. surge data gives probabilities that the observed 2017–22 clustering is a product of random sampling of ~15%, for Alaska/Yukon against RGI-extended <1%, for Svalbard (against both RGI and Farnsworth data) of ~97% and for HMA (against RGI and Guillet data) close to 100 and 64%, respectively. This indicates that the Alaska/Yukon surges 2017–22 are likely clustered within their region. The 2017–22 HMA surges are weakly clustered and only when considering the (more systematic) Guillet data. The 2017–22 Svalbard surges show no statistically significant clustering within their region.

Fifty-six glaciers from the 2017–22 dataset are marked as surge-type in RGI v.6, while the remaining 59 glaciers are not. Twenty-eight of these 59 2017–22 surges have in RGI v.6 the flag 'observed', 11 have 'probable', seven have 'possible' and nine have 'no evidence' (RGI-Consortium, 2017). It is important

https://doi.org/10.1017/jog.2023.35 Published online by Cambridge University Press

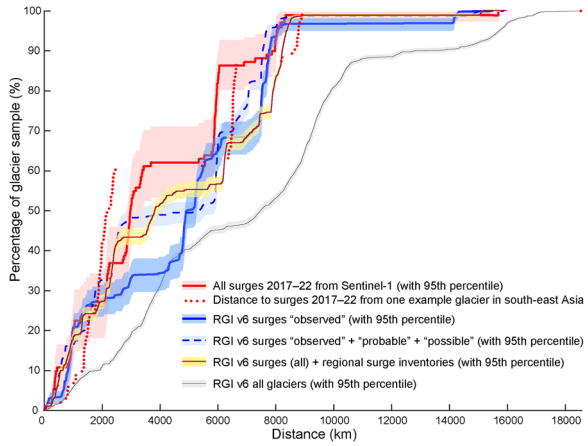

Figure 3. Average distance of any 2017–22 glacier surge to all other 2017–22 surging glaciers, given as percentage of the entire sample (empirical cumulative distribution function, eCDF, of distances between 115 glaciers, red curve). Similar distributions for different subsamples of RGI v.6 glaciers with surge indication (blue curves) and an own extension of RGI v.6 surges by selected regional surge inventories (brown curve; see text for details). The higher on the *y*-axis and the more stepped a curve appears, the more spatial clustering of the sample it indicates. For illustration, the distance distribution of one surging glacier (Sedongpu Glacier; 94.9 lon, 29.8 lat, south-east Asia) to all other 2017–22 surging glaciers is also given (each glacier one red dot). Note, in contrast to the other average and thus continuous distributions, the latter distances from one single glacier are measured to 114 individual other glaciers and thus represented as dots rather than lines. For reference, the eCDF of distances is also given for all RGI v.6 glaciers (216'502 glaciers, black curve). The difference between the black and blue or red curves, respectively, is however not of interest as it displays the well-known fact of general global surge clustering. Regional eCDF curves for Alaska/Yukon, Svalbard and HMA are included in the Supplementary material.

to note that this comparison refers to same RGI IDs. In particular for large glaciers and glacier systems with one common RGI ID, coincident IDs from our survey and the RGI do not necessary mean it is the same glacier tributary that surged. Similarly, in our 2017–22 data, the same RGI ID can occur several times (up to three times) due to different tributaries of the same large RGI glacier having surged during that time. The transfer of the surge data from Sevestre and Benn (2015) into RGI involved a similar aggregation (RGI-Consortium, 2017). Therefore, some care is required when basing surge statistics on RGI IDs only.

Over HMA, our Sentinel-1 backscatter-based inventory contains 68 surges during 2017–2022. Most glaciers in our dataset are also included in Guillet and others (2022) which we consulted independently after compilation of our dataset. Our data contain four RGI-IDs and 25 GLIMS-IDs that are not included in the Guillet and others (2022) dataset. Our study uses GLIMS IDs as main glacier identifier, Guillet and others (2022) use RGI IDs as main identifier. Many larger glaciers in HMA are aggregated as one RGI ID but consist of several smaller glacier units with individual GLIMS IDs. As for RGI surge flags, we can thus not be sure if the same tributaries surged, even if the RGI IDs agree. Guillet and others (2022) and our study barely overlap temporally and use different surge identifiers and surge definitions, as is discussed in more detail in the following section. Compared to the 708 surge-type glaciers on Svalbard listed by Farnsworth and others (2016) our dataset contains three new surge-type glaciers.

To initially test for potential mass balance signals of our 2017–22 surge-type glaciers, we intersect our dataset with the global 2000–20 glacier volume changes from Hugonnet and others (2021) (cf. Guillet and others, 2022). We compare the elevation change rate of each of our 2017–22 surge data with the one of all glaciers around it within a radius of 50 km that are not surging and have no RGI surge indication. We do this analysis both for 2010–20 and 2000–20 elevation changes from Hugonnet and others (2021). On average, the surging glaciers show a more negative elevation change than the surrounding non-surging ones, but the difference is within the standard deviations of both samples (2010–20: mean elevation change surging -0.43 ± 0.59 m a^{-1}, non-surging: -0.26 ± 0.25 m a^{-1}; 2000–20: surging -0.24 ± 0.41 m a^{-1}, non-surging: -0.19 ± 0.23 m a^{-1}). Closer examination exhibits that the majority of surging glaciers in this analysis have a similar elevation change rate than non-surging glaciers (cf. Guillet and others, 2022). Only ten surging glaciers lost up to three times more elevation than the surrounding ones, causing a more negative overall average. Analysing these ten glaciers in more detail shows, however, that they are different from their surrounding non-surging neighbours and thus difficult to compare. In particular, they have significantly lower elevation range and slope, and are situated at lower elevation. For such low-lying low-angle glaciers, some of which are tidewater calving glaciers, mass balance would be expected to be comparably negative anyway, independent of surge-type activity. Examining the relation between glacier mass balance and surging closer than done here would have to consider the surge phase of the individual glaciers, e.g. when the surge started and ended. In particular, our study detects by design no surge-type glaciers during quiescent phase, which is however an important part of the mass-balance cycle of such glaciers. It is open to discussion whether all surge-type glaciers that did not surge during 2017–22 should automatically be defined as being in quiescent phase.

Discussion

Potential and limitations of the approach

The novel method to map surge-type events globally and at annual scale from repeat satellite radar images appears quite robust and well suited for this purpose (Leclercq and others, 2021). We cannot be sure to have mapped every such event that happened over 2017–22, but a large number of cross-checks with literature, own data (velocity time series, optical satellite data, frontal advance, elevation changes), and discussion with colleagues makes us confident that we have identified a large percentage of events that qualify as surges with significant backscatter changes. For quantification of our identification success rate over two test regions based on velocity data, see Leclercq and others (2021) who found full agreement with velocity data qualitatively indicating surges on Svalbard, and large velocity increases for seven out of eight surge-like events over Alaska/Yukon with increasing backscatter (see also Samsonov and others, 2021). Here, we in addition compare our results to surges over HMA from Guillet and others (2022). From the 90 surges with time stamps of 2017 and 2018 (derived from ITS_LIVE velocity data) in the latter study, our data agree with 22 surges. For two surges in 2017 and 2018 from Guillet and others (2022) we find that we overlooked surge-type backscatter changes in Sentinel-1 data, mostly because of major topographic effects (layover, foreshortening) or complex signals of the cases. During the careful comparison of our dataset with the one by Guillet and others (2022) we discovered two more surge-type backscatter changes without 2017 and 2018 time stamps in the latter dataset. Also these cases are characterised by major topographic effects and weak backscatter signals. For completeness, we include these four surges in the final version of our dataset. For the remaining ~65 cases by Guillet and others with 2017–18 time stamp, we do not find any backscatter changes or in few cases only very weak ones that we purposely excluded previously. We find two main reasons for these disagreements. First, where involving ice speed changes in assigning surge characteristics, Guillet and others (2022) use the amplitude of intra-annual speed variations relative to the average long-term ice speeds, in

https://doi.org/10.1017/jog.2023.35 Published online by Cambridge University Press

addition to at least one other indicator from peculiar elevation changes and visual surge indications. This latter approach includes many comparable slow and long-lasting surge-like processes, a type of ice-flow instability that our backscatter approach typically is not sensitive to as it detects mainly large changes between subsequent years. (A future implementation of our approach could look into multi-year backscatter changes or backscatter variations within the entire Sentinel-1 stack instead of annual stacks.) Second, the difference in approaches by us and Guillet and others and thus the different surge indications applied is not only a methodological one, but it reflects also a fundamental range in surge definitions in terms of amplitude and duration of (speed) changes that are certainly open to discussion, including the definition of when a surge starts and ends.

As investigated closer for HMA, missed events are likely due to surges that did not lead to significant changes in crevassing and thus backscatter, or for very small glaciers in steep rough terrain with topographic disturbances of recorded backscatter. We could also have missed events in our visual interpretation of backscatter changes, errors that we try to minimise by compiling three independent surveys. Finally, it is important to stress that our definition of surge-type activity is based on backscatter changes and does thus not necessary agree with other definitions used for surge-type activity and other indicators as listed above in the introduction section. Our approach appears to coincide well with large changes (most clearly with increases) in ice speed (Fig. 1 and Leclercq and others, 2021), visual interpretations of enhanced crevassing in optical images and glacier advances due to surges, which typically also become visible in the approach of this study. A detailed comparison between surge velocity time series and radar backscatter in order to kinematically characterise backscatter changes remains to be done, though.

Features such as looped moraines or specific landforms in the glacier forefield (e.g. Farnsworth and others, 2016) indicate past surge activity rather than ongoing one. By design, the approach to detect surges from backscatter changes cannot detect such retrospective indicators. Similarly, the kinematic approach of this study cannot detect specific patterns of elevation change that can be associated with surge-type activity, such as build-up of accumulation zones during the quiescent phase or drainage of accumulation zones and thickening of tongues during the surge active phase (Guillet and others, 2022). Our approach is thus different, and potentially complementary, to other (semi-) automatic approaches of surge characterisation and mapping. Herreid and Truffer (2016), for instance, use deformations of moraine features to find and characterise glacier speed variations. On the substantive surges we map such features are typically destroyed, if present at all. On the other hand, as explained above for HMA, our approach is not well suited to detect more subtle surge-like processes. Vale and others (2021) support their surge identification by detection of particularly large glacier length changes. As surge-related terminus advances are often accompanied by terminus crevassing, our approach is also able to detect such processes. Our inherent surge definition does however not directly encompass glacier advance (or retreat) as indicator. On the other hand, our approach works also for surges that do not involve glacier length changes, such as tributary surges. Ke and others (2022) base surge detection on particular changes in normalised difference snow index in 500 m resolution multispectral data. Though only suitable for comparably large glaciers and less connected to glacier kinematics, their approach could in parts be sensitive to similar processes as our approach, such as increased reflectance from pronounced glacier advance or disruption of debris cover. The approach also provides surge timing. Bouchayer and others (2022) use statistical approaches (machine learning) to classify surge-type glaciers on Svalbard. From the 25 glaciers surging during 2017–22 according to our data, three to four mostly small and narrow ones have a surge probability of smaller 50% in the automated classification.

Inventory of surge events 2017–2022 and uncertainties

Compared to the analysis of 2018–19 Sentinel-1 data contained in Leclercq and others (2021), our data for 2018–2019 contain 14 fewer surges. We considered these to be too uncertain to be listed as clear surges when analysing the entire 2017–22 time series (list given in the Supplementary material). The uncertainties associated with the interpretation of some of them as surge-type events are discussed in more detail in Leclercq and others (2021). In the current study, we included only very clear surge-type backscatter changes and rather left out subtle signs of surging such as from slow and long-lasting surge-like processes. The longer time period investigated here enabled also to examine the temporal consistence of surge signs over several years. Compared to Leclercq and others (2021), our study includes 50 new surges, 20 of which have already RGI surge indication and 30 not yet.

We cannot give quantitative uncertainties for our surge detections as they are based on visual interpretations. The comparison between our three individual mappings suggests that the majority of cases appears as clear surge-type backscatter change but also that ~20% of the cases need closer examination or are overlooked in some of the mappings. This highlights a need for some training and harmonisation between operators prior to backscatter-based surge identification. As we have conservatively chosen to include only very clear signals in our final dataset we consider the probability for false positives to be low (glaciers falsely identified as surging). The probability for false negatives (undetected surges) is certainly higher. We consider the largest sources of such omissions to be (i) subtle surges where slow and long-term speed changes limit the evolution of clear crevasse changes between subsequent years, (ii) surges of already strongly crevassed glaciers or glacier parts, (iii) surges that may not result in major crevassing or perhaps only along lateral margins, (iv) substantive changes in glacier surface properties such as snow cover or snow melt conditions that could overprint backscatter changes from crevasses, for instance by filling of crevasses by snow in one year but not another, and (v) simply overlooking surge signs in our visual survey. From our comparisons to velocity data we also find that decreasing backscatter can in general less clearly be connected to surge behaviour. This is not surprising as the crevasse disappearance is a process that is less directly linked to surge cessation than crevasse formation is to surge emergence. In the Supplementary material we list five example cases of potentially surge-like backscatter changes that we considered to be too uncertain to include in our final list. Our comparisons in Leclercq and others (2021) and above against Guillet and others (2022) indicate that the omissions from overlooking clear backscatter surge signs should be far below 10% of the cases that are in principle detectable by our approach. We consider that a main uncertainty in our surge detection stems from surge definition (start, end, magnitude, temporal characteristics, indicators, etc.), and when comparing to other studies, from the uncertainty of localisation of the surge within a glacier system consisting of several tributaries.

Global clustering

Our examination of the distance distributions using bootstrapping and the 95th percentiles of the cumulative distance distribution functions, both investigated on global and regional levels, indicates two main geo-statistical factors behind the stronger clustering of our 2017–22 data relative to the RGI surge data. First and

https://doi.org/10.1017/jog.2023.35 Published online by Cambridge University Press

most important, the global surge clusters in the Canadian and Russian Arctic, and Greenland/Iceland showed no or only very few surges between 2017 and 2022. Second, within the cluster Alaska/Yukon our 2017–22 data are relatively more concentrated than the reference distributions of surge-type glaciers used here. We would however like to note that in particular RGI v.6 and our RGI-extended is globally inhomogeneous and within regions biased due to uneven spatial coverage and different surge definitions and detection methods used for different regions.

A main question that arises from our new data is how the particular spatial clustering during 2017–22 can be interpreted. The short time-scale of 5 years compared to typical surge cycle periods of decades implies that the clustering could not be statistically significant. Only longer time series will enable to separate these factors from each other with certainty, and it remains to be seen over which time-scales the global clustering found here remains. Our bootstrapping test suggests statistical significance for the clustering on global level, but in most cases not on regional levels. Relative to the RGI v.6 surge-type glaciers (blue curves in Fig. 3) the clustering of surge activity during 2017–2022 might in reality be even larger when we assume that the RGI surge flags are already more spatially clustered than the real distribution of surges because the existing RGI surge flags are based on individual studies over selected areas of special research focus, a selection which most likely introduces clustering rather than a consistent global-scale distribution. A potential bias in the observed clustering could in theory also stem from a spatial bias in our surge detection. For instance, surges could in some regions systematically be of a nature that limits pronounced backscatter changes such as a regional tendency to low-magnitude long-lasting subtle surges. Despite the constraints due to the shortness of our observation period and a potential regional detection bias it is also possible to interpret the observed clustering as a consequence of meteorological or climatic impacts (Sevestre and Benn, 2015; Benn and others, 2019; Hock and others, 2019). Such impacts can result in locally enhanced ice melt (Dunse and others, 2015; Yasuda and Furuya, 2015) or snow-fall/snow-melt anomalies, with direct impacts on glacier mass balance (Kienholz and others, 2017; Gilbert and others, 2018) or thermal regimes (Murray and others, 2003; Nuth and others, 2019). Synchronous surges of nearby glaciers have been reported before for smaller areas and meteorological/climatic drivers named as possible factors (e.g. Eisen and others, 2001; Pitte and others, 2016; Kääb and others, 2018; Chudley and Willis, 2019; Paul and others, 2022). Potential meteorological or climatic factors on surging can act on a range of time scales. For instance, the 2017–22 global surge clustering could be a short-term response (delay in the order of years or less), or a long-term response reflecting forcing that happened decades ago. Also, instead of interpreting the 2017–22 global surge clustering as a response to external forcing, one could in an inverse way rather interpret the near-absence of surges in some other regions in terms of climate impacts. Earlier clustering of surges in regions without current surges could, for instance, have synchronised surge cycles in a way that these glaciers did not have restored enough mass to surge again, even under a forcing that triggered surging elsewhere. Our method of systematic and global monitoring of surge-type events and registering surge timing (something that is not included in RGI so far and would have to be recovered from the original literature) demonstrates a way to address the question of climate influence on glacier surging on multiannual to decadal time scales.

We also run the cluster analysis for sub-periods of 2017–22, but conclude that our 5-year observation period is too short to draw meaningful conclusions regarding surge initiation time and duration, except for the well-known fact that surge-type activities can span over time scales of a few months to several years. Comparing the 10- and 20-year elevation change rate of the surging glaciers of our study to surrounding non-surging glaciers exhibits no significant difference, or at least no difference that could be clearly attributed to glacier surging. This type of analysis could be extended, though, by a more detailed consideration of surge timing and phase with respect to the period of observed elevation changes in order to characterise any temporal variations in elevation change rates in response to surging.

We did not carefully map or investigate the backscatter changes on outlet glaciers of the Greenland ice sheet, but note that at least for some of the glaciers contained in Table S3 available literature suggests indeed distinct acceleration or deceleration events (e.g. Upernavik Isstrøm central (Derkacheva, 2021), Harald Moltke Bræ (Müller and others, 2021)). This indicates that analysing Sentinel-1 backscatter time series can also be a useful avenue to complement remote-sensing-based velocity measurements over outlet glaciers.

Conclusions

Based on radar backscatter changes over time, we infer surge-type glacier activity from marked changes in glacier crevassing. Our 2017–22 map of surge-type events is to our best knowledge the first globally consistent time-stamped inventory of active surges. Even if our approach is not perfect and we might have missed surge-type events, a number of checks and validations suggest the approach is robust. The approach implies a definition of surging that is at least in parts different from the ones used traditionally, a property of our inventory that could cause inconsistencies with other datasets of surge-type glaciers. We also find that the localisations of surge events according to entire glacier systems versus tributaries within them complicate comparisons between different surge inventories (and the extraction of meaningful glacier parameters).

We find 115 surge-type events in the period of 2017–22. Hundred of these happened on glaciers that have already been known as surge-type, according to the RGI v.6 and the other reference studies used here. Our data show a distinct clustering of surge-type events in three regions, namely (i) Karakoram, Pamirs and West Kunlun Shan (~50 surges), (ii) Svalbard (~25) and (iii) the Kluane National Park and Reserve/St. Elias Mountains (~9). Other regions that contain surge-type glaciers (e.g. reported in RGI) did not host glacier surges in 2017–22, or only a few scattered ones. This clustering on global level may point to large-scale meteorological or climatic influences on surge timing, but our 5-year observation period is too short to exclude with certainty other possible effects such as random interference of surge cycles or spatial biases in our surge detection approach.

Our study opens up a number of further applications. For instance, other special cryospheric events such as lake outbursts, avalanches, calving events or changes on ice-sheet outlet glaciers can be mapped using our method (see also Leclercq and others, 2021). Further potential applications of our data include complementing other approaches to identify surges (e.g. Guillet and others, 2022), initiating closer investigation of specific surges, better understanding or modelling of surge distribution in time and space or improved consideration of surges in climate-related glacier analyses. Attempts could be undertaken to support or replace our visual surge detection by automatic procedures, and to combine it with automatic detection of substantial ice speed changes (Herreid and Truffer, 2016; Guillet and others, 2022). Eventually, we envision that our approach of surveying major radar backscatter changes on glaciers (also, but not only from surges) can be

https://doi.org/10.1017/jog.2023.35 Published online by Cambridge University Press

developed into an element of operational global-scale monitoring of cryospheric changes, both forward in time based on upcoming SAR data and back in time based on existing SAR data archives.

Supplementary material. The supplementary material for this article can be found at https://doi.org/10.1017/jog.2023.35.

Acknowledgements. We thank the editor Hester Jiskoot, and the referees Martin Truffer and Tobias Bolch for their knowledgeable and helpful comments on the manuscript. Robert McNabb and Frank Paul gave additional valuable hints to surge glacier inventories. This research has been supported by ESA through Glaciers CCI and Earth Explorer 10 Harmony studies (grant nos. 4000127593/19/I-NB and 4000135083/21/NL/FF/ab). The study is also a contribution to the Svalbard Integrated Arctic Earth Observing System SIOS and the MAMMAMIA project (RCN grant no. 301837). The collection of data for this study was mainly done using Google Earth Engine (https://earthengine.google.com), the data analyses using ArcGIS and Matlab software, and Randolph Glacier Inventory (https://nsidc.org/data/nsidc-0770/versions/6) and GLIMS (http://www.glims.org) data were used for reference. The study is based on EU Copernicus Sentinel-1 data, provided by EU/ESA (https://scihub.copernicus.eu).

Author contributions. A. K.: conceptualisation, methodology, software, investigation, validation, analysis, writing. V. B. and P. L.: methodology, software, investigation, writing. E. M. and T. S.: investigation, validation, writing.

References

Altena B, Scambos T, Fahnestock M and Kääb A (2019) Extracting recent short-term glacier velocity evolution over southern Alaska and the Yukon from a large collection of Landsat data. *The Cryosphere* **13**(3), 795–814. doi: 10.5194/tc-13-795-2019

Benn DI, Fowler AC, Hewitt I and Sevestre H (2019) A general theory of glacier surges. *Journal of Glaciology* **65**(253), 701–716. doi: 10.1017/jog.2019.62

Bevington A and Copland L (2014) Characteristics of the last five surges of Lowell Glacier, Yukon, Canada, since 1948. *Journal of Glaciology* **60**(219), 113–123. doi: 10.3189/2014JoG13J134

Bhambri R, Hewitt K, Kawishwar P and Pratap B (2017) Surge-type and surge-modified glaciers in the Karakoram. *Scientific Reports* **7**(1), 15391. doi: 10.1038/s41598-017-15473-8

Bouchayer C, Aiken JM, Thogersen K, Renard F and Schuler TV (2022) A machine learning framework to automate the classification of surge-type glaciers in Svalbard. *Journal of Geophysical Research-Earth Surface* **127**(7), Artn e2022JF006597. doi: 10.1029/2022JF006597

Chudley TR and Willis IC (2019) Glacier surges in the north-west West Kunlun Shan inferred from 1972 to 2017 Landsat imagery. *Journal of Glaciology* **65**(249), 1–12. doi: 10.1017/jog.2018.94

Copland L, Sharp MJ and Dowdeswell JA (2003) The distribution and flow characteristics of surge-type glaciers in the Canadian High Arctic. *Annals of Glaciology* **36**(36), 73–81. doi: 10.3189/172756403781816301

Copland L and 8 others (2009) Glacier velocities across the central Karakoram. *Annals of Glaciology* **50**(52), 41–49. doi: 10.3189/172756409789624229

Derkacheva A (2021) *Seasonal Flow Variability of Greenlandic Glaciers: Satellite Observations and Numerical Modeling to Study Driving Processes* (PhD). Université Grenoble Alpes, Grenoble, France.

Dunse T and 5 others (2015) Glacier-surge mechanisms promoted by a hydro-thermodynamic feedback to summer melt. *The Cryosphere* **9**(1), 197–215. doi: 10.5194/tc-9-197-2015

Eisen O, Harrison WD and Raymond CF (2001) The surges of Variegated Glacier, Alaska, USA, and their connection to climate and mass balance. *Journal of Glaciology* **47**(158), 351–358. doi: 10.3189/172756501781832179

Farnsworth WR, Ingolfsson O, Retelle M and Schomacker A (2016) Over 400 previously undocumented Svalbard surge-type glaciers identified. *Geomorphology* **264**, 52–60. doi: 10.1016/j.geomorph.2016.03.025

Gardelle J, Berthier E, Arnaud Y and Kääb A (2013) Region-wide glacier mass balances over the Pamir-Karakoram-Himalaya during 1999–2011. *The Cryosphere* **7**(4), 1263–1286. doi: 10.5194/tc-7-1263-2013

Gilbert A and 8 others (2018) Mechanisms leading to the 2016 giant twin glacier collapses, Aru Range, Tibet. *The Cryosphere* **12**(9), 2883–2900. doi: 10.5194/tc-12-2883-2018

Goerlich F, Bolch T and Paul F (2020) More dynamic than expected: an updated survey of surging glaciers in the Pamir. *Earth System Science Data* **12**(4), 3161–3176. doi: 10.5194/essd-12-3161-2020

Gorelick N and 5 others (2017) Google Earth Engine: planetary-scale geospatial analysis for everyone. *Remote Sensing of Environment* **202**, 18–27. doi: 10.1016/j.rse.2017.06.031

Grant KL, Stokes CR and Evans IS (2009) Identification and characteristics of surge-type glaciers on Novaya Zemlya, Russian Arctic. *Journal of Glaciology* **55**(194), 960–972. doi: 10.3189/002214309790794940

Guan WJ and 7 others (2022) Updated surge-type glacier inventory in the West Kunlun mountains, Tibetan Plateau, and implications for glacier change. *Journal of Geophysical Research-Earth Surface* **127**(1), Artn e2021JF006369. doi: 10.1029/2021JF006369

Guillet G and 6 others (2022) A regionally resolved inventory of High Mountain Asia surge-type glaciers, derived from a multi-factor remote sensing approach. *Cryosphere* **16**(2), 603–623. doi: 10.5194/tc-16-603-2022

Guo L and 5 others (2022) A new inventory of High Mountain Asia surge-type glaciers derived from multiple elevation datasets since the 1970s. *Earth System Science Data Discussions*, [preprint], in review. doi: 10.5194/essd-2022-238

Harrison WD and Post AS (2003) How much do we really know about glacier surging? *Annals of Glaciology* **36**, 1–6. doi: 10.3189/172756403781816185

Herreid S and Truffer M (2016) Automated detection of unstable glacier flow and a spectrum of speedup behavior in the Alaska Range. *Journal of Geophysical Research-Earth Surface* **121**(1), 64–81. doi: 10.1002/2015jf003502

Hock R and 14 others (2019) High mountain areas. In Pörtner H-O, Roberts DC, Masson-Delmotte V, Zhai P, Tignor M, Poloczanska E, Mintenbeck E, Alegría A, Nicolai M, Okem A, Petzold J, Rama B and Weyer NM (eds), *IPCC Special Report on the Ocean and Cryosphere in a Changing Climate (SROCC)*. Cambridge, UK and New York, USA: Cambridge University Press, pp. 131–202.

Hugonnet R and 10 others (2021) Accelerated global glacier mass loss in the early twenty-first century. *Nature* **592**(7856), 726–731. doi: 10.1038/s41586-021-03436-z

Jacquemart M and 7 others (2020) What drives large-scale glacier detachments? Insights from Flat Creek glacier, St. Elias Mountains, Alaska. *Geology* **48**(7), 703–707. doi: 10.1130/g47211.1

Jiskoot H (2011) Glacier surging. In Singh VP, Singh P and Haritashya UK (eds), *Encyclopedia of Snow, Ice and Glaciers*. Dordrecht, The Netherlands: Springer, pp. 415–428.

Jiskoot H, Murray T and Luckman A (2003) Surge potential and drainage-basin characteristics in East Greenland. *Annals of Glaciology* **36**, 142–148. doi: 10.3189/172756403781816220

Kääb A and 18 others (2018) Massive collapse of two glaciers in western Tibet in 2016 after surge-like instability. *Nature Geoscience* **11**(2), 114–120. doi: 10.1038/s41561-017-0039-7

Kääb A and 14 others (2021) Sudden large-volume detachments of low-angle mountain glaciers. More frequent than thought? *The Cryosphere* **15**(4), 1751–1785. doi: 10.5194/tc-15-1751-2021

Ke LH, Zhang JS, Fan CY, Zhou JJ and Song CQ (2022) Large-scale monitoring of glacier surges by integrating high-temporal- and -spatial-resolution satellite observations: a case study in the Karakoram. *Remote Sensing* **14**(18), Artn 4668. doi: 10.3390/rs14184668

Kienholz C, Hock R, Truffer M, Bieniek P and Lader R (2017) Mass balance evolution of Black Rapids Glacier, Alaska, 1980–2100, and its implications for surge recurrence. *Frontiers in Earth Science* **5**, Artn 56. doi: 10.3389/feart.2017.00056

Leclercq PW, Kääb A and Altena B (2021) Brief communication: detection of glacier surge activity using cloud computing of Sentinel-1 radar data. *The Cryosphere* **15**(10), 4901–4907. doi: 10.5194/tc-15-4901-2021

Muhammad S and 8 others (2021) A holistic view of Shisper Glacier surge and outburst floods: from physical processes to downstream impacts. *Geomatics Natural Hazards & Risk* **12**(1), 2755–2775. doi: 10.1080/19475705.2021.1975833

Mukherjee K and 6 others (2017) Surge-type glaciers in the Tien Shan (Central Asia). *Arctic Antarctic and Alpine Research* **49**(1), 147–171. doi: 10.1657/Aaar0016-021

Müller L and 8 others (2021) Surges of Harald Moltke Brae, north-western Greenland: seasonal modulation and initiation at the terminus. *The Cryosphere* **15**(7), 3355–3375. doi: 10.5194/tc-15-3355-2021

Murray T, Strozzi T, Luckman A, Jiskoot H and Christakos P (2003) Is there a single surge mechanism? Contrasts in dynamics between glacier surges in Svalbard and other regions. *Journal of Geophysical Research-Solid Earth* **108** (B5), Artn 2237. doi: 10.1029/2002jb001906

Nuth C and 9 others (2019) Dynamic vulnerability revealed in the collapse of an Arctic tidewater glacier. *Scientific Reports* **9**(1), 5541. doi: 10.1038/s41598-019-41117-0

Paul F and 25 others (2015) The glaciers climate change initiative: methods for creating glacier area, elevation change and velocity products. *Remote Sensing of Environment* **162**, 408–426. doi: 10.1016/j.rse.2013.07.043

Paul F and 9 others (2022) Three different glacier surges at a spot: what satellites observe and what not. *The Cryosphere* **16**(6), 2505–2526. doi: 10.5194/tc-16-2505-2022

Pitte P and 7 others (2016) Geometric evolution of the Horcones Inferior Glacier (Mount Aconcagua, Central Andes) during the 2002–2006 surge. *Journal of Geophysical Research-Earth Surface* **121**(1), 111–127. doi: 10.1002/2015jf003522

Rankl M and Braun M (2016) Glacier elevation and mass changes over the central Karakoram region estimated from TanDEM-X and SRTM/X-SAR digital elevation models. *Annals of Glaciology* **57**(71), 273–281. doi: 10.3189/2016AoG71A024

RGI-Consortium (2017) Randolph Glacier Inventory version 6. GLIMS Technical Report. Available at https://nsidc.org/sites/nsidc.org/files/technical-references/RGI_Tech_Report_V6.0.pdf

Round V, Leinss S, Huss M, Haemmig C and Hajnsek I (2017) Surge dynamics and lake outbursts of Kyagar Glacier, Karakoram. *The Cryosphere* **11**(2), 723–739. doi: 10.5194/tc-11-723-2017

Samsonov S, Tiampo K and Cassotto R (2021) Measuring the state and temporal evolution of glaciers in Alaska and Yukon using synthetic-aperture-radar-derived (SAR-derived) 3D time series of glacier surface flow. *The Cryosphere* **15**(9), 4221–4239. doi: 10.5194/tc-15-4221-2021

Sevestre H and Benn DI (2015) Climatic and geometric controls on the global distribution of surge-type glaciers: implications for a unifying model of surging. *Journal of Glaciology* **61**(228), 646–662. doi: 10.3189/2015JoG14J136

Steiner JF, Kraaijenbrink PDA, Jiduc SG and Immerzeel WW (2018) Brief communication: the Khurdopin glacier surge revisited – extreme flow velocities and formation of a dammed lake in 2017. *The Cryosphere* **12**(1), 95–101. doi: 10.5194/tc-12-95-2018

Strozzi T, Luckman A, Murray T, Wegmuller U and Werner CL (2002) Glacier motion estimation using SAR offset-tracking procedures. *IEEE Transactions on Geoscience and Remote Sensing* **40**(11), 2384–2391. doi: 10.1109/Tgrs.2002.805079

Strozzi T, Paul F, Wiesmann A, Schellenberger T and Kääb A (2017) Circum-Arctic changes in the flow of glaciers and ice caps from satellite SAR data between the 1990s and 2017. *Remote Sensing* **9**(9), Artn 947. doi: 10.3390/rs9090947

Thogersen K, Gilbert A, Schuler TV and Malthe-Sorenssen A (2019) Rate-and-state friction explains glacier surge propagation. *Nature Communications* **10**, Artn 2823. doi: 10.1038/s41467-019-10506-4

Truffer M and 10 others (2021) Chapter 13 – glacier surges. In Haeberli W and Whiteman C (eds), *Snow and Ice-Related Hazards, Risks, and Disasters*, 2nd Edn. Amstersdam, The Netherlands: Elsevier, pp. 417–466.

Vale AB, Arnold NS, Rees WG and Lea JM (2021) Remote detection of surge-related glacier terminus change across High Mountain Asia. *Remote Sensing* **13**(7), Artn 1309. doi: 10.3390/rs13071309

Yasuda T and Furuya M (2015) Dynamics of surge-type glaciers in West Kunlun Shan, Northwestern Tibet. *Journal of Geophysical Research-Earth Surface* **120**(11), 2393–2405. doi: 10.1002/2015JF003511

https://doi.org/10.1017/jog.2023.35 Published online by Cambridge University Press